Superconductor-semiconductor interaction effects in mesoscopic hybrid structures

F. Rahman, T. J. Thornton, and R. Huber*
Department of Electrical and Electronic Engineering, Imperial College, Exhibition Road, London SW7 2BT, United Kingdom

L. F. Cohen, W. T. Yuen, and R. A. Stradling
Department of Physics, Imperial College, Prince Consort Road, London SW7 2AZ, United Kingdom
(Received 20 May 1996)

We have studied transport in mesoscopic superconductor-semiconductor hybrid structures consisting of two-dimensional arrays of micrometer-sized niobium dots deposited on high-mobility InAs:GaSb quantum wells. The grating arrays were designed to have a dot size and spacing of 3, 1.5, and 1 μm, so as to be smaller than the electron mean free path of $\sim$5 μm. At low temperatures all the structures show clear evidence of Andreev reflection while the two smaller period samples also exhibit a proximity-induced superconducting phase. We present measurements of the differential resistance at different temperatures and magnetic fields. For fields greater than 0.3 T, different features are observed in the differential resistance which we attribute to nonuniform flux penetration around the superconducting dots. [S0163-1829(96)00444-4]

INTRODUCTION

Superconductor-semiconductor (Su-Se) hybrid systems have been under investigation for more than a decade now. Recently, it has become possible to study structures in which transport through the semiconductor occurs over distances shorter than the mean free path and phase-coherence length, the so-called mesoscopic regime. These structures have the potential to clarify issues relating to the proximity effect[1] and Andreev reflection.[2] The proximity effect refers to the induction of superconductivity in an otherwise normal material by the evanescent decay of the order parameter from a superconducting phase in close proximity. Andreev reflection is a process in which electrons below the superconducting energy gap are reflected as holes back into the normal material with a transfer of charge $2e$ into the superconductor. An exciting possibility is the exploitation of the proximity effect in transistorlike structures.[3–6] Although practical devices have yet to emerge, a variety of physical phenomena have been observed.[7–15]

The work described here is based on investigations carried out on mesoscopic hybrid structures consisting of arrays of superconducting niobium dots with periodicities of a few microns, deposited on InAs/GaSb quantum wells. Both Andreev reflection and the proximity effect have been studied but in ways which differ from other more conventional approaches. Instead of active current injection through superconducting contacts, a current is made to flow through a two-dimensional electron gas (2DEG) over which mesoscopic structures are patterned. The current therefore enters the superconductor from the semiconductor and not vice versa. The systems studied have multiple junctions patterned as a regular array of micrometer-sized isolated dots. Our results demonstrate the existence of both Andreev reflection and the proximity effect and we present a systematic investigation of how each varies with temperature and magnetic field.

DEVICE FABRICATION

High quality InAs/GaSb quantum wells with typical electron concentration of 1×10^{12} cm^{-2} and electron mobilities in the range 250 000–300 000 cm^2/V s (both at 4.2 K) were used in this work.[16–18] The layer structure consisted of a 200-Å InAs well sandwiched between an upper 200-Å GaSb barrier layer and a bottom 8000-Å GaSb barrier layer. Underneath the bottom barrier layer was an 8000-Å-thick layer of epitaxial GaAs serving as a buffer layer. The whole structure was grown by MBE on (001) semi-insulating GaAs. The InAs:GaSb material system has associated with it the advantages of high electron concentration, high-mobility, and ease of formation of low contact resistance Ohmic contacts with the InAs channel.

The quantum well material was patterned into Hall bar structures by optical lithography and wet etching. Electrical contacts were made to the Hall bar using a Ni/Au metalization. The Hall bars were 80 μm wide and had voltage probes spaced by 200 μm. For each Hall bar two portions of the channel could be probed independently and in this way results from different geometrical arrays deposited under identical conditions could be compared (see Fig. 1). Alternatively, a portion of the Hall bar could be left unpatterned to confirm the properties of the quantum well. Various arrays of

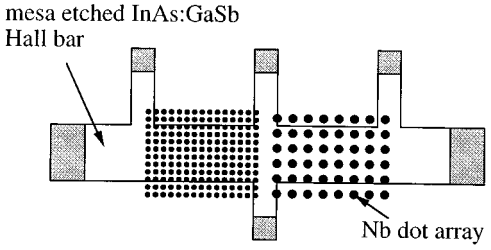

FIG. 1. A schematic illustration of the Su-Se hybrid structures used in this work.

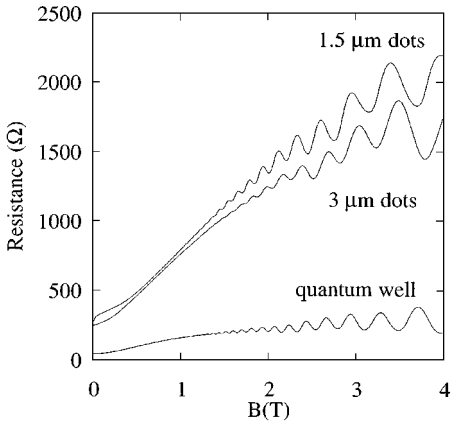

FIG. 2. A comparison of the magnetoresistance of an unpatterned InAs:GaSb quantum well and a hybrid structure patterned with a 3- and 1.5-μm dot array. $T=0.4$ K in each case.

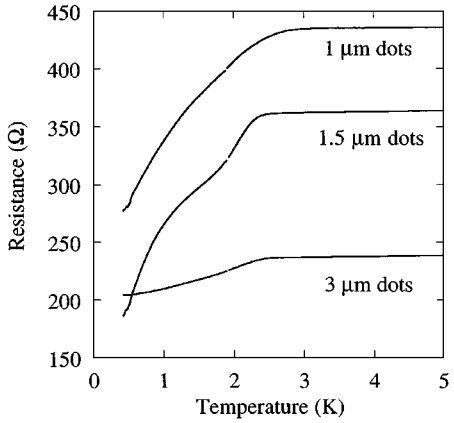

FIG. 3. The temperature dependence of the resistance for three different dot arrays with dot size and separations of 3, 1.5, and 1 μm. The break in the data below 2 K is due to a changeover to a more sensitive thermometer.

dots were patterned between different pairs of voltage probes by electron-beam lithography.

Niobium (Nb) has become the superconductor of choice for Su-Se hybrid devices. When properly deposited, a specific contact resistance as low as 5×10^{-7} Ω cm^2 has been measured for Nb-InAs contacts.[19] We used wet chemical etching to selectively remove the GaSb prior to Nb deposition. This step removed the GaSb, exposing the underlying InAs only where Nb had to be deposited so that the quantum well was left intact between the Nb dots. Just before Nb deposition, a low voltage dc glow discharge sputter cleaning was carried out to remove any native oxide and wet etch residues from the exposed InAs surfaces. This process is crucial for obtaining high-quality Su-Se contacts and therefore must be very carefully controlled. An approximately 100-nm-thick layer of niobium was deposited on the exposed InAs by electron-beam assisted thermal evaporation and lift off. Full details of the fabrication process are given elsewhere.[20]

The gratings patterned in the manner described above were designed such that the separation between the center of two adjacent dots was twice the dot diameter. For all of the samples the array of dots uniformly covered the entire 200×80 μm^2 channel between the voltage probes and the total area of niobium deposited on the quantum well is therefore the same for each grating. We present below results from three different gratings with dot diameters, a, of 3, 1.5, and 1 μm. The 3 and 1.5 μm gratings were adjacent to each other on the same Hall bar. The 1-μm grating was adjacent to an unpatterned region of the quantum well on another device.

It is important to confirm that the quantum well regions between the niobium dots are not damaged by the processing. Overetching of the GaSb will lead to an excessive undercut while lateral damage from the sputter cleaning can reduce the electron mobility. In Fig. 2, the magnetoresistance taken from a Hall bar patterned with the 3- and 1.5-μm gratings is compared to that from a similar Hall bar made from an unpatterned quantum well from the same wafer. From the periodicity of the Shubnikov–de Haas oscillations the electron concentration in the quantum well, n, is 1.35×10^{12} cm^{-2} and it has a sheet resistance of 17.5 Ω/square. The electron mobility and mean free path in the unpatterned quantum well are, therefore, 265 000 cm^2/V s and 5 μm, respectively. The electron concentration in the regions patterned with the dot arrays is 1.05×10^{12} cm^{-2} and the oscillations appear at fields above 1 T. This is in marked contrast to the case where all the GaSb is first removed by chemical etching, after which the current flows in an accumulation layer at the exposed InAs surface. The electron concentration in the surface 2DEG is typically 2.5×10^{12} cm^{-2} and the oscillations are only observed for fields in excess of 2 T, indicating the reduced mobility of carriers at the exposed surface. Although the lithography and subsequent processing used to deposit the gratings does seem to slightly reduce the electron concentration, it is clear from the data in Fig. 2 that the quantum well in between the dots is left intact and that the mean free path is probably not significantly reduced compared to the value of 5 μm measured in the unpatterned well.

RESULTS AND DISCUSSION

Upon cooling to 10 K, the resistances of the 3-, 1.5-, and 1-μm devices were found to be 235, 360, and 435 Ω, respectively, and were almost independent of temperature for $T>3$ K, as indicated in Fig. 3. The observed trend, i.e., an increased resistance for reduced dot separation, is worthy of comment. The area of Nb covered InAs and unpatterned quantum well is the same for each grating and we might therefore expect the total resistance to be the same. However, this neglects any contact resistance associated with current flowing into and out of the Nb, which may well be more significant in gratings with a larger number of dots.

On further cooling the Nb became superconducting, with a broad transition starting at 2.4 K. The T_c of bulk Nb is 9.8 K and the reduced value that we observe is attributed to impurity incorporation during film deposition which reduces the superconducting energy gap, 2Δ, from 3 meV to $\sim$0.8 meV. Below 2.4 K the temperature dependence of the resistance, $R(T)$, is qualitatively different for the portion of the Hall bar patterned with 3-μm dots as compared to those patterned with smaller diameter dots. For the region with 3-μm dots $R(T)$ appears to saturate at a value of 205 Ω (see Fig.

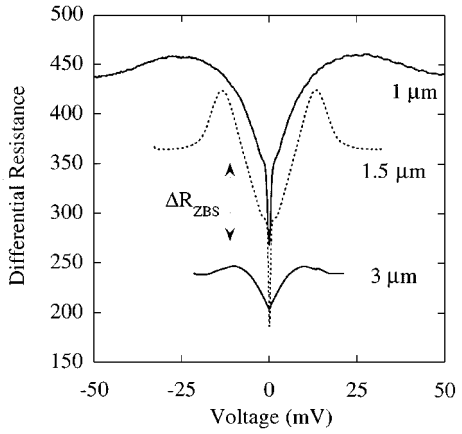

FIG. 4. The differential resistance as a function of applied bias at a base temperature of 0.4 K.

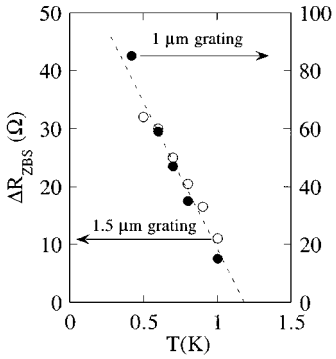

FIG. 5. The magnitude of the zero-bias resistance spike ΔR_{ZBS} at different temperatures for the 1.5-μm grating (open circles) and the 1-μm grating (full circles). The dashed line is a guide to the eye indicating that ΔR_{ZBS} vanishes at a temperature of $\sim$1.2 K for both hybrid structures.

3). For the 1.5-μm dots, however, $R(T)$ begins to decrease rapidly below 1 K and continues decreasing even down to the lowest temperatures measured. The $R(T)$ behavior for another hybrid device patterned with 1-μm diameter dots showed qualitatively similar behavior to that with 1.5-μm dots despite being deposited on a different Hall bar on a separate occasion. We believe these results can be explained in terms of a transition from Andreev mediated transport to a proximity-induced supercurrent transport as T decreases. As the Nb first turns superconducting, i.e., for $T \leqslant 2.4$ K, the resistance of the sample begins to drop due to the conductivity enhancement resulting from Andreev reflection. If this were the only transport mechanism we would expect the resistance to saturate at a finite value when extrapolating to zero temperature as is indeed the case for the 3-μm sample. For the 1.5- and 1-μm samples the reduced separation between the dots makes it possible for a proximity-induced supercurrent to flow in the InAs between the dots and at a low enough temperature we would expect to observe a vanishingly small resistance between the voltage probes.

Further evidence in support of the transport mechanisms that we propose above can be obtained from the differential resistance measurements plotted in Fig. 4. The most pronounced feature for each of the graphs are the symmetrically disposed shoulders and the broad resistance dip around zero bias which we attribute to Andreev reflection. Andreev reflection has been observed in numerous Su-Se hybrid systems where the current is forced to flow across the Su-Se interface by applying a bias across the contacts. In our hybrid devices the current is injected into the semiconductor by means of normal electrodes which are placed mm's away from the active region. The current flows in a region of the Hall bar which is patterned with the periodic array of dots. In samples where we have not removed the GaSb or not argon sputtered the InAs surface prior to Nb deposition the dV/dI curves are essentially featureless. Only when the surface is suitably prepared will the transmission across the interface be large enough to observe Andreev reflection. The most striking difference between the plots is the presence of a sharp zero-bias spike (ZBS) in the differential resistance spectrum of the 1.5- and 1-μm devices. We take this as evidence for interdot proximity coupling which results in a proximity precursor that sharply lowers the resistance near zero bias. Using a value of $0.025 m_e$ for the effective mass of electrons in the InAs well, we obtain $\xi_N = (\hbar^2/2\pi m^* kT)(2\pi n)^{1/2} = 3.5$ μm for the coherence length in InAs, in the clean limit[21] at $T = 0.4$ K. This length scale is consistent with our observation of a well-developed lateral proximity coupling in the 1.5 and 1-μm dot lattices, but not in the one with a 3-μm separation. Differential resistance dips referred to as zero-bias anomalies have been observed in the past by several research groups who have proposed explanations for the phenomenon ranging from the proximity effect[12,22] to constructive quantum interference due to coherent Andreev reflection.[6,7,23] A pronounced zero-bias anomaly, observed as a sharp peak in the differential conductance, has been reported by Nguyen, Kroemer, and Hu[8] and was attributed to multiple Andreev reflection under the niobium contact electrodes. This feature survived up to the critical temperature of the niobium film, which is a quite different behavior from the temperature dependence of the ZBS that we observe, as described below.

A study of the evolution of differential resistance spectrum with changes in temperature shows that while Andreev reflection is not very sensitive to temperature in the 0.4–1 K region explored, the ZBS is highly temperature dependent. We plot the magnitude of the zero-bias spike, ΔR_{ZBS} (as indicated in Fig. 4), against temperature in Fig. 5. Extrapolation indicates that the ZBS disappears completely at a temperature above 1.2 K. At temperatures lower than this, proximity coupling reduces the resistance of the hybrid structure and explains the rapid decrease in resistance (see Fig. 3). We note here that the amplitude of the ZBS decreased over a period of weeks, presumably due to a degradation in the quality of the Nb/InAs interface. The data from the 1.5-μm array shown in Fig. 5 were taken almost six weeks after the corresponding data in Fig. 4 were recorded. During this time the amplitude of the ZBS had decreased by approximately 50%. The data from the 1-μm array shown in Figs. 4 and 5 were recorded on the same day, but a repeat of the measurement some weeks later showed that the ZBS in this device had also decreased significantly ($\Delta R_{\mathrm{ZBS}} \sim 20$ Ω at $T = 0.4$ K). Only the features associated with the ZBS showed any long term time dependence—those associated with Andreev re-

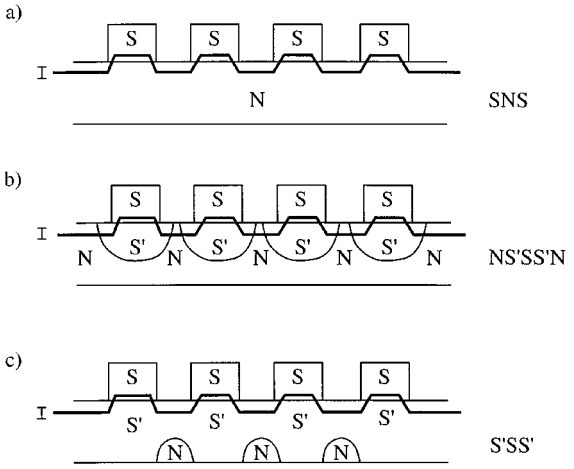

FIG. 6. Schematic diagram of the transport current path across the Nb/InAs interface at (a) $1.2<T<2.4$ K for $V\ll 2\Delta$ of S, (b) $0.4<T<1.2$ K for $V\ll 2\Delta$ of S', and (c) $T\ll 0.4$ K for $V<2\Delta$ of S'. Here S indicates that the Nb is superconducting and S' and N indicate the proximity and normal regions, respectively, in the InAs.

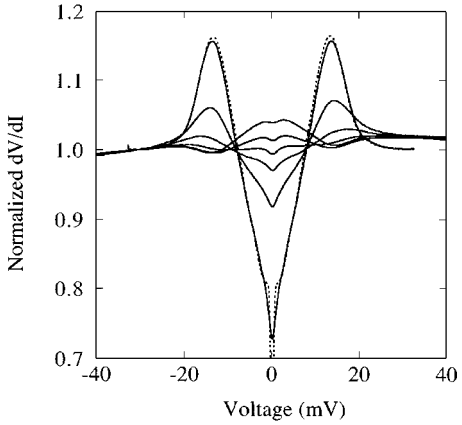

FIG. 7. The differential resistance normalized to the value at −30 mV as a function of applied bias. The magnetic fields used in the measurements are 0 T for the dashed line and 0.3, 0.5, 0.8, 1.0, 1.2, and 1.5 T for the solid lines with increasing field corresponding to increasing zero-bias normalized resistance. $T=0.4$ K.

flection were reproducible over a period of many months during which these experiments were performed. Because of the decay in the amplitude of the ZBS it is hard to make meaningful comparisons between the numerical values of ΔR_{ZBS}. However, the amplitude of the ZBS extrapolates to zero at a temperature of ~1.2 K when measured shortly after fabrication (as in the case of the 1-μm array) or some weeks later (in the case of the 1.5-μm array). This suggests that the ZBS originates from a proximity-induced superconducting phase with a $T_C\sim 1.2$ K rather than from multiple Andreev reflection which would be expected to survive to higher temperatures.[8]

It is important to understand exactly where the current flows in the hybrid structure at different temperatures and current bias values. In Fig. 6 one scenario is illustrated schematically. For $1.2<T<2.4$ K, if the normal superconductor (NS) interface is clean enough the current will be diverted across the interface and into the superconductor. The structure will resemble a multiple array of $\ldots NSN\ldots$ junctions connected in series and parallel [Fig. 6(a)]. At high enough bias current the superconductor will become resistive making the detour of the current path increasingly improbable. For $0.4<T<1.2$ K, regions of the InAs will have become superconducting by proximity and the current will flow across $NS'SS'N$ junctions [Fig. 6(b)]. Again this picture is only valid for low enough bias. For $T\ll 0.4$ K, the entire InAs layer immediately below the dot array will be superconducting and the hybrid structure will resemble series of $S'SS'$ junctions in parallel [Fig. 6(c)]. The signature for this behavior would be a pure supercurrent flowing across the entire system (i.e., the differential resistance would go to zero for $V=0$), which was not observed in our experiments.

Our measurements of dV/dI vs V suggest that the $NS'SS'N$ picture most accurately describes our hybrid structures. The main evidence for this interpretation comes from the width of the Andreev reflection dip which approximately scales with the number of dot columns along the grating. The 3-, 1.5-, and 1-μm gratings have 34, 68, and 96 columns of dots and the corresponding widths between the shoulders of the Andreev reflection dip at 0.4 K are 18, 27, and 51 mV, respectively. Assuming that each dot takes part in the current transport, we arrive at an average energy scale of 0.49 ± 0.05 meV for each $NS'SS'N$ junction in the array. Current flowing through each dot has to pass through two NS' junctions and the value that we expect for 2Δ is, therefore, approximately 0.25 meV. This value is approximately three times smaller than the value of 2Δ that we estimate for the niobium film itself but the relevant superconductor for the Andreev reflection is the proximity-induced phase, S', which is expected to have a smaller energy gap due to the discontinuous drop in the order parameter at the InAs:Nb interface.[1]

In Fig. 7 we plot the differential resistance for magnetic fields up to 1.5 T for the sample with a 1.5-μm dot array. The values have been normalized to the value measured at ~30 mV so as to clearly show the zero-bias behavior. The device with a 3-μm array behaves in a qualitatively similar fashion, as shown in Fig. 8. The 1-μm device broke down before it could be used for these measurements. We find that for both devices measured the $NS'SS'N$ picture of the grating hybrids is also consistent with their magnetic-field behavior. An important point is that a continuous film of niobium deposited on InAs with a $T_c=3.9$ K had a critical current of 1 mA at 0.4 K in zero magnetic field and a critical magnetic field (H_{c2}) of 3 T at 0.4 K. Therefore, we expect that in the case of the dot structure, when $B\ll 1$ T at 0.4 K, the flux will be mostly screened out from the niobium regions. The flux density across the dot array will be extremely nonuniform with the regions between the dots having considerably higher-flux density. Our measurements show that the proximity-induced ZBS is destroyed by an applied field as small as 10 mT, while the features due to Andreev reflection remain essentially unchanged for fields up to 300 mT (see Fig. 7). For small applied fields most of the flux will be expelled from the superconducting niobium resulting in an increased flux density between the dots. Only for fields larger than 300 mT does enough flux penetrate the niobium to influence the Andreev reflection and reduce the amplitude of the peaks in the 10–20 mV bias range.

For applied fields up to 300 mT the dominant features

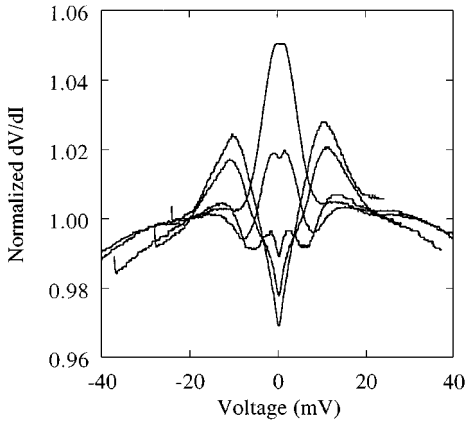

FIG. 8. Same as Fig. 7 for the 3-μm grating. The magnetic fields used were 0.5, 0.8, 1.0, 1.2, and 1.5 T and the data were normalized to the value at -20 mV.

shown in Figs. 7 and 8 are reminiscent of Andreev reflection. However, at larger fields a new structure begins to develop at biases smaller than ± 10 mV. At 500-mT, points of inflection have developed for the 1.5-μm sample and, as the field is increased, the features develop into pronounced peaks. The peaks occur at a voltage, $V_{\max}$, which varies with B, but is typically less than a few mV's either side of zero bias. A similar structure develops for the device with a 3-μm grating but at smaller magnetic fields. The results shown in Figs. 7 and 8 have not, to the best of our knowledge, been observed in SNS devices in which current is injected into a semiconductor via superconducting electrodes. Nitta, Akazaki, and Takayanagi[24] used a Nb-InAs-Nb device which showed a structure in the dV/dI vs V curves for biases less than $2\Delta/e$. The structure was attributed to multiple Andreev reflection but saturated for fields less than 5 mT. Interestingly, Marsh, Williams, and Ahmed[15] have observed Andreev reflection up to 2.5 T in a GaAs sample with alloyed tin contacts but with no indication of a resistance maxima at zero bias.

The bias point at which the differential peaks occur, $V_{\max}$, follows an approximately $1/B$ behavior ($V_{\max} \sim B^{-1.0}$ for the 3-μm grating and $B^{-1.1}$ for the 1.5-μm grating) indicating that the cyclotron length, $L_c = \hbar k_F / eB$ may determine the underlying physics. However, for fields greater that 0.5 T where the new peaks are strongly developed, the cyclotron length $L_c \leqslant 0.33$ μm which is much smaller than the periodic features of any of the gratings. For this reason it is difficult to conceive of an orbital or geometrical effect that could lead to the clear resistance peaks that we observe at $\pm V_{\max}$. For a given magnetic field $V_{\max}$ is approximately 3.3 times larger in the sample with 1.5-μm diameter dots and spacing compared to that with dimensions of 3 μm. Taking into account the nonuniformity in the flux density the difference is sufficiently close to the factor of 4 difference in the area of quantum well between the dots suggesting that the position of $V_{\max}$ is determined by the intensity of the field penetrating the quantum well between the dots. However, for the 1-μm sample the flux penetration is more than 70 h/e which is much larger than the few flux quanta ($\varnothing_0 = h/e$) required to modify the quantum interference.[11] On the other hand, the flux is sufficient to produce Landau-level quantization in the 2DEG, as evidenced by the Shubnikov–de Haas oscillations which can be resolved for fields above 0.8 T. The Landau-level quantization will dramatically alter the density of states in the 2DEG which in turn will effect the transmission across the normal-superconducting (NS) interface. Blonder, Tinkham and Klapwijk[25] have calculated the transmission through an NS junction as a function of the barrier height, Z, at the interface. Andreev reflection and a reduced zero-bias resistance corresponds to a vanishingly small barrier i.e., $Z = 0$ and as Z increases a resistance maximum develops indicating that quasiparticle tunneling is the dominant transport mechanism for high barrier junctions. Our data presented in Figs. 7 and 8 show a pronounced transition from a resistance minima to a resistance maxima as B increases. This behavior is consistent with the formation of a barrier at the NS interfaces but more work is needed before we can attribute the data to Landau-level quantization.

CONCLUSION

In summary, this paper has described work on mesoscopic hybrid structures consisting of a regular two-dimensional array of niobium dots deposited on the InAs of an InAs:GaSb quantum well. For arrays with interdot separations of 1.5 and 1.0 μm the hybrid devices showed a resistive transition with different slopes in the R versus T plot signaling gross changes in the superconducting configuration of the structure. The change in slope of resistance with temperature coincides with the appearance of a sharp dip in the differential resistance at small-bias voltages. This zero-bias spike (ZBS), which is absent in dot lattices with dot separations larger than 3 μm, is a manifestation of interdot proximity effect. The ZBS was found to be very sensitive to temperature and the proximity-induced superconducting phase vanishes for temperatures above 1.2 K. The Andreev reflection is almost independent of magnetic field for $B \leqslant 0.3$ T, but for higher fields new features are observed in the differential resistance measurements.

ACKNOWLEDGMENTS

We would like to thank Professor David Caplin for his support of the project. We wish to thank Tanveer Mallick, Carsten Gatzke, and Jasper Nehls for sharing their experience of the properties and processing of InAs/GaSb quantum wells. We also thank Dr. David Williams of the Hitachi Cambridge Laboratory for useful discussions. The support of CVCP in providing an ORS award is gratefully acknowledged. This work was supported by the EPSRC.

*Present address: University of Basel, Institute of Physics, Klingelbergstrasse 82, CH-4056 Basel, Switzerland.

[1] P. G. de Gennes, Rev. Mod. Phys. **36**, 225 (1964).
[2] A. F. Andreev, Zh. Eksp. Teor. Fiz. **46**, 1823 (1964) [Sov. Phys. JETP **19**, 1228 (1964)].
[3] T. D. Clark *et al.*, J. Appl. Phys. **51**, 2736 (1980).
[4] A. W. Kleinsasser *et al.*, Appl. Phys. Lett. **55**, 1909 (1989).
[5] J. Nitta *et al.*, Phys. Rev. B **46**, 14 286 (1992).
[6] T. Akazaki *et al.*, Appl. Phys. Lett. **68**, 418 (1996).
[7] B. van Wees *et al.*, Phys. Rev. Lett. **69**, 510 (1992).

[8] C. Nguyen, H. Kroemer, and E. L. Hu, Phys. Rev. Lett. **69**, 2847 (1992).
[9] H. Takayanagi, J. Hansen, and J. Nitta, Phys. Rev. Lett. **74**, 166 (1995).
[10] W. Huffelen *et al.*, Phys. Rev. B **47**, 5170 (1993).
[11] I. K. Marmokos, C. Beenakker, and R. Jalabert, Phys. Rev. B **48**, 2811 (1993).
[12] S. Chaudhuri and P. F. Bagwell, Phys. Rev. B **51**, 16 936 (1995).
[13] A. Kastalsky *et al.*, Phys. Rev. Lett. **67**, 3026 (1991).
[14] T. Nishino, E. Yamada, and U. Kawabe, Phys. Rev. B **33**, 2042 (1986).
[15] A. Marsh, D. Williams, and H. Ahmed, Semicond. Sci. Technol. **10**, 1694 (1995); Physica B **203**, 307 (1994).
[16] T. Malik, S. Chung, J. J. Harris, A. G. Norman, R. A. Stradling, and W. T. Yuen, *International Conference on Narrow Gap Semiconductors (Santa Fe)*, IOP Conf. Proc. No. 144 (Institute of Physics and Physical Society, London, 1995), p. 229.
[17] M. W. Wang *et al.*, Appl. Phys. Lett. **66**, 2981 (1995).
[18] H. Munekata, E. E. Mendez, Y. Iye, and L. Esaki, Surf. Sci. **174**, 449 (1986).
[19] C. Nguyen *et al.*, Appl. Phys. Lett. **65**, 103 (1994).
[20] R. Huber, F. Rahman, T. J. Thornton, A. Norman, and R. A. Stradling (unpublished).
[21] G. Deutscher and P. G. de Gennes, in *Superconductivity*, edited by R. D. Parks (Marcel Dekker, New York, 1969), Vol. 2, p. 1005.
[22] N. Agrait, J. Rodrigo, and S. Vieira, Phys. Rev. B **46**, 5814 (1992).
[23] P. H. C. Magnée *et al.*, Phys. Rev. B **50**, 4594 (1994).
[24] J. Nitta, T. Akazaki, and H. Takayanagi, Phys. Rev. B **49**, 3659 (1994).
[25] G. Blonder, M. Tinkham, and T. Klapwijk, Phys. Rev. B **25**, 4515 (1981).